J. Phys. D: Appl. Phys., Vol. 6, 1973. Printed in Great Britain.

Pressures and stresses in freezing water drops

W D King and N H Fletcher
Department of Physics, University of New England, Armidale, New South Wales 2351, Australia

Received 7 May 1973

Abstract. Calculations of the pressure in the liquid core of a freezing water droplet and stresses in the surrounding ice shell are made. The theory is developed in terms of two mechanical models for the ice. The first model assumes it is elastic and the second that it is linearly viscoelastic. The calculated pressure development is compared with that measured in drops one centimetre in diameter. It is concluded that the viscoelastic theory is sufficient for describing the pressure growth, but overestimates the magnitudes of the stresses in the shell. It is suggested that a treatment using a non-linear dependence of strain rate on stress would yield a more realistic stress distribution.

1. Introduction

It has been known for some time that in strongly convective clouds the number of ice crystals can exceed the number of ice nuclei by several orders of magnitude (Mossop 1970). One of the earliest mechanisms proposed to explain the anomaly was the shattering of freezing water droplets. It was envisaged that, as the droplet froze inwards, the expansion of water would cause sufficient pressure to fragment the shell. Subsequent experimental investigations have shown that this is unlikely to be of importance in clouds (Hobbs and Alkezweeny 1968, Brownscombe and Thorndike 1968), but there is no theory available with which the experiments can be compared.

In this paper we compute the pressures in the liquid core and stresses in the shell of a freezing droplet. The first approach assumes that the ice shell is elastic, and the second that it is viscoelastic. The effects of droplet size, freezing time, and the rheological properties of ice on the calculations are discussed. Finally, we present the results of experiments in which pressures were measured and discuss these in terms of the theory.

Although the discussion is given in terms of the freezing of water droplets, the theory also applies to the freezing of droplets of any liquid which expands on solidfying. Additional examples of such materials are germanium, silicon, and certain organic substances.

2. Elastic shell theory

Water droplets which are cooled slowly normally supercool to a temperature characterized by the size and nature of insoluble particles present. When the ice phase is nucleated by these particles, dendrites of ice grow very rapidly through the drop and continue to do so until the latent heat evolved warms the droplet to 0 °C. This dendritic growth stage lasts for a time of the order of milliseconds and results in a fraction $\Delta T/80$ of the

droplet being frozen, where ΔT is the supercooling. Further growth of ice is then determined by heat transfer to the environment.

In the following treatment we have assumed that the heat transfer is spherically symmetric, so that a uniform shell forms and grows inward. We have not considered the asymmetry introduced by the dendrites, and have assumed the ice is homogeneous and isotropic and used the corresponding elastic theory.

It is worth noting that the standard Lamé treatment of a spherical shell subjected to an internal pressure (Sokolnikoff 1956, pp 343–4) cannot be used. In the present problem the pressure build-up and shell growth are inter-related, whereas in the Lamé treatment these are quite independent. In the droplet problem, the innermost layer of the shell is in equilibrium with the pressure, and the stresses in this layer are then modified by the effects of subsequent growth. In form, it is similar to adding prestressed layers to the inside of the shell. Consequently, the main distinction between the Lamé and droplet problems is that a release of pressure in the latter does not reduce the shell to a state of zero stress.

The model used to compute the pressure is as follows. Consider a partially frozen droplet with the interface at the radial position ξ. In time δt, suppose the shell grows inward by an amount $\delta\zeta$ determined by the heat transfer, and suppose the inside of the shell already formed moves out by an amount δu under the influence of the increased pressure. The net result is that the interface has moved by an amount

$$\delta\xi=\delta\zeta+\delta u \tag{1}$$

where all three coordinates are measured in the positive radial direction.

The change in volume of the liquid core is given by

$$\delta V=4\pi(1-\Delta T/80)\,\xi^2(\alpha\delta\zeta+\delta u) \tag{2}$$

where $\alpha=1-\rho_{\text{ice}}/\rho_{\text{water}}$. Because water is more compressible than ice, α increases with pressure, but since fracture normally occurs at less than 100 bar, the variation in α is less than 4% in this range, and we have treated it as a constant. The increase in internal pressure P is then given by

$$\delta P=\frac{-3B}{\xi}\,(\alpha\delta\zeta+\delta u) \tag{3}$$

where $B=\beta(1-\Delta T/80)$ and β is the bulk modulus of water. We may rewrite this in terms of the interfacial position using equation (1), giving

$$\frac{\mathrm{d}P}{\mathrm{d}\xi}=\frac{-3B}{\xi}\left(\alpha+(1-\alpha)\,\frac{\partial u}{\partial\xi}\bigg|_{r=\xi}\right). \tag{4}$$

The determination of the pressure thus requires that the elastic displacement field $u(r,\xi)$ be known. The symmetry is such that for the stress components $\tau_{\alpha\beta}$

$$\left.\begin{aligned}&\tau_{r\theta}=\tau_{r\phi}=\tau_{\theta\phi}=0\\&\tau_{\theta\theta}=\tau_{\phi\phi}\end{aligned}\right\} \tag{5}$$

and similarly for the strain components $e_{\alpha\beta}$.

The equations describing the elastic behaviour of the shell are as follows (Sokolnikoff 1956, pp 71–2). First there is the condition for equilibrium

$$\frac{\mathrm{d}\tau_{rr}}{\mathrm{d}r}=\frac{2}{r}\,(\tau_{\theta\theta}-\tau_{rr}) \tag{6}$$

and then the stress–strain relations. It is convenient to write these in the form

$$e_{rr}+2\,e_{\theta\theta}=\frac{\tau_{rr}+2\tau_{\theta\theta}}{3k} \tag{7}$$

$$e_{rr}-e_{\theta\theta}=\frac{\tau_{rr}-\tau_{\theta\theta}}{2\mu} \tag{8}$$

where k and μ are the moduli of compression and rigidity respectively. For small strains we can write

$$\left.\begin{aligned} e_{rr}&=\frac{\partial u(r)}{\partial r}\\ e_{\theta\theta}&=\frac{u(r)}{r}\end{aligned}\right\} \tag{9}$$

and these sets of equations, (6)–(9), can be combined to give Navier's equation for spherical symmetry:

$$\frac{\mu}{r^2}\frac{\partial}{\partial r}\left(r^2\frac{\partial u}{\partial r}\right)+\left(\frac{3k-2\mu}{3}\right)\frac{\partial}{\partial r}\left(\frac{\partial u}{\partial r}+\frac{2u}{r}\right)=0 \tag{10}$$

for which the solution is (Sokolnikoff 1956, pp 343–5)

$$u(r,\xi)=\frac{f(\xi,a)r}{3k}+\frac{g(\xi,a)}{4\mu r^2} \tag{11}$$

where the explicit dependence of the functions f and g has been indicated, and a is the drop radius.

The stress components can be obtained from the displacement field by equations (7), (8) and (9) and are

$$\tau_{rr}(r,\xi)=f(\xi,a)-\frac{g(\xi,a)}{r^3} \tag{12}$$

and

$$\tau_{\theta\theta}(r,\xi)=f(\xi,a)+\frac{g(\xi,a)}{2r^3}. \tag{13}$$

Simple manipulation of equations (12) and (13) shows that f is a measure of the hydrostatic pressure at any point, and g/r^3 a measure of the shearing stresses.

Equations (11), (12) and (13) have been obtained by neglecting the stress history of the shell, and the treatment is formally the same as that for the Lamé situation. The present problem is concerned with the increments in the stresses and displacement as the shell grows inward, however, and it is the form of the functions $f(\xi,a)$ and $g(\xi,a)$ and the way in which these incremental stresses are superposed which lend this problem its distinctiveness.

The increments in stresses and displacements can be obtained by differentiating equations (11), (12) and (13) with respect to ξ:

$$\frac{\partial u}{\partial\xi}(r,\xi)=\frac{r}{3k}\frac{\partial f}{\partial\xi}+\frac{1}{4\mu r^2}\frac{\partial g}{\partial\xi} \tag{14}$$

$$\frac{\partial\tau_{rr}}{\partial\xi}(r,\xi)=\frac{\partial f}{\partial\xi}-\frac{\partial g}{\partial\xi}\frac{1}{r^3} \tag{15}$$

and

$$\frac{\partial \tau_{\theta\theta}}{\partial \xi}(r, \xi) = \frac{\partial f}{\partial \xi} + \frac{\partial g}{\partial \xi}\frac{1}{2r^3} \tag{16}$$

where we have neglected such terms as $(\partial f/\partial a)\,(\mathrm{d}a/\mathrm{d}\xi)$ because $\mathrm{d}a/\mathrm{d}\xi \ll 1$, the movement of the outer boundary being very small compared with that of the inner.

At the outer boundary, the pressure can be taken to be zero, while at the inner boundary the newly frozen layer is in equilibrium with the pressure, so that

$$\tau_{rr}(a) = 0; \quad \tau_{rr}(\xi) = -P(\xi). \tag{17}$$

Further, the increase in pressure due to subsequent growth acts on the completed shell, the changes in stresses being determined by the form of the functions $f(\xi, a)$ and $g(\xi, a)$. Therefore

$$\tau_{rr}(r, \xi) = -P(r) + \int_r^{\xi} \frac{\partial \tau_{rr}}{\partial \xi}\,\mathrm{d}\xi \tag{18}$$

and similarly for $\tau_{\theta\theta}$.

In fact, the right-hand expressions ought to be evaluated at a point we shall call r', where r' is the initial point which is subsequently displaced out to r. The replacement of r' by r is equivalent to interchanging the geometrical coordinates with the ice coordinates—that is, the position of a given element of ice. The differences so caused are negligible because the elastic strains remain small. Even on the outer boundary, where the approximation is worst, the error is less than 1%.

The functions $\partial f/\partial \xi$ and $\partial g/\partial \xi$ can be determined from the boundary conditions

$$\left.\frac{\partial \tau_{rr}}{\partial \xi}\right|_{r=a} = 0 \tag{19}$$

and

$$\left.\frac{\partial \tau_{rr}}{\partial \tau}\right|_{r=\xi} = -\frac{\partial P}{\partial \xi}. \tag{20}$$

Although intuitively obvious, equation (20) can be obtained rigorously by substituting the integral forms for τ_{rr} and $\tau_{\theta\theta}$ (equation (18)) into the equilibrium equation (6). These last two equations can be rewritten, using equations (4), (14) and (15), as

$$\frac{\partial f}{\partial \xi} - \frac{\partial g}{\partial \xi}\frac{1}{a^3} = 0 \tag{21}$$

and

$$\frac{\partial f}{\partial \xi} - \frac{1}{\xi^3}\frac{\partial g}{\partial \xi} = \frac{3B}{\xi}\left[\alpha + (1-\alpha)\left(\frac{\xi}{3k}\frac{\partial f}{\partial \xi} + \frac{1}{4\mu\xi^2}\frac{\partial g}{\partial \xi}\right)\right] \tag{22}$$

for which the solutions are

$$\frac{\partial g}{\partial \xi} = \frac{12\mu B\alpha k}{\xi}\left[\frac{4\mu\{k - B(1-\alpha)\}}{a^3} - \frac{k\{4\mu + 3B(1-\alpha)\}}{\xi^3}\right]^{-1} \tag{23}$$

and

$$\frac{\partial f}{\partial \xi} = \frac{12\mu B\alpha k}{a^3\xi}\left[\frac{4\mu\{k - B(1-\alpha)\}}{a^3} - \frac{k\{4\mu + 3B(1-\alpha)\}}{\xi^3}\right]^{-1}. \tag{24}$$

Using these expressions, we can evaluate $\partial \tau_{rr}/\partial \xi$, $\partial \tau_{\theta\theta}/\partial \xi$ and $\partial P/\partial \xi$. Integration over

the appropriate limits then yields the quantities

$$P(\xi)=-3B\alpha \lg\left(\frac{\xi}{a}\right)-\frac{B^2\alpha(1-\alpha)}{[k-B(1-\alpha)]}\lg\left(1+\frac{4\mu[k-B(1-\alpha)]\,[1-\xi^3/a^3]}{B(1-\alpha)\,(4\mu+3k)}\right)$$
$$-\frac{3B^2\alpha(1-\alpha)}{[4\mu+3B(1-\alpha)]}\lg\left(1+\frac{k[4\mu+3B(1-\alpha)]\,[(a^3/\xi^3)-1]}{B(1-\alpha)\,(4\mu+3k)}\right) \tag{25}$$

$$\tau_{rr}(r,\xi)=-P(r)-\frac{kB\alpha}{[k-B(1-\alpha)]}\left(\frac{a^3}{r^3}-1\right)$$
$$\times\lg\left(1+\frac{4\mu\,[k-B(1-\alpha)]\,[(r/a]^3-(\xi/a)^3]}{k[4\mu+3B(1-\alpha)]-4\mu\,[k-B(1-\alpha)]\,(r/a)^3}\right) \tag{26}$$

$$\tau_{\theta\theta}(r,\xi)=-P(r)+\frac{kB\alpha}{[k-B(1-\alpha)]}\left(\frac{a^3}{2r^3}+1\right)$$
$$\times\lg\left(1+\frac{4\mu\,[k-B(1-\alpha)]\,[(r/a)^3-(\xi/a)^3]}{k[4\mu+3B(1-\alpha)]-4\mu\,[k-B(1-\alpha)]\,(r/a)^3}\right). \tag{27}$$

These expressions, which are shown by the curves labelled $n=0$ in figures 1–5, present the solution for the stresses in the frozen shell on the assumption of ideal elastic behaviour. The values used for the elastic constants are those found by Gold (1958) for polycrystalline ice at -5 °C. Several points are worthy of special comment.

(i) $P(\xi)\to\infty$ as $\xi\to 0$. This is expected since the inner radius of curvature of the shell then approaches zero.

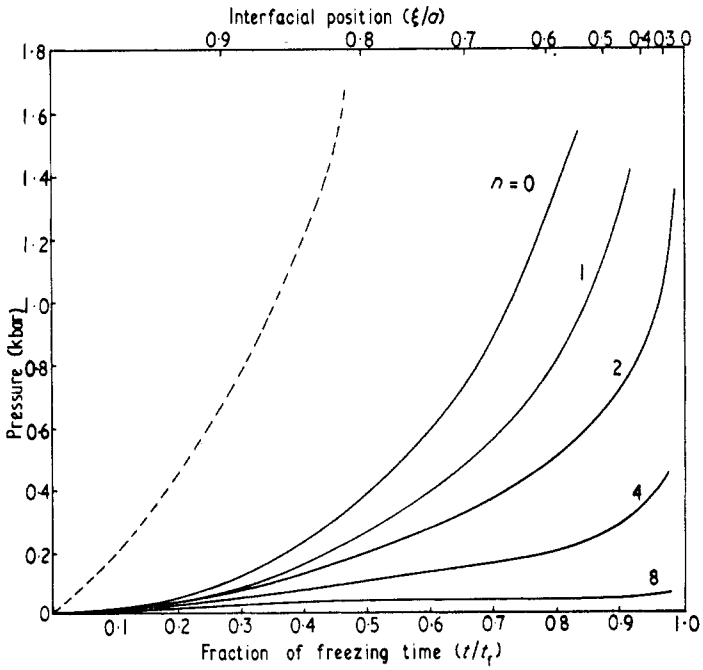

Figure 1. Calculated pressures as a function of time and interfacial position for various values of the viscoelastic parameter n. The curve (— — —) is calculated for a rigid shell, and the elastic shell is described by $n=0$.

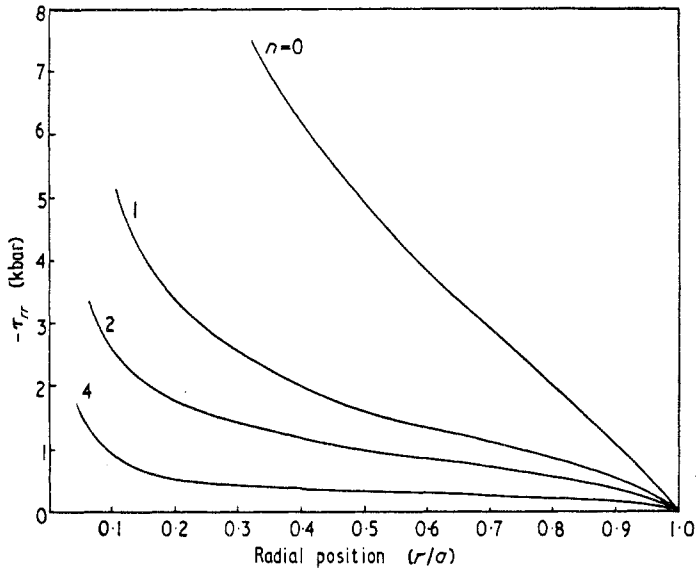

Figure 2. Variation of τ_{rr} with radial position in a frozen droplet. The elastic curve is given by $n=0$.

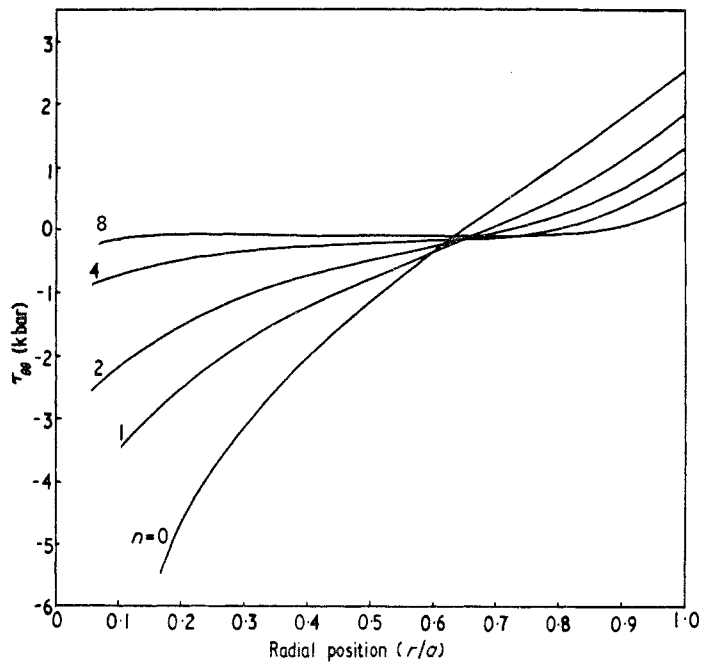

Figure 3. Variation of $\tau_{\theta\theta}$ with radial position in a frozen droplet. The elastic curve is given by $n=0$.

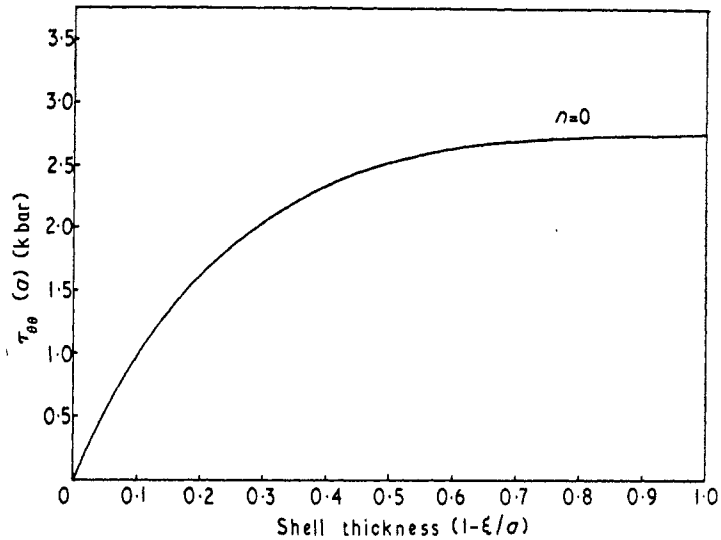

Figure 4. $\tau_{\theta\theta}$ on the surface as a function of shell thickness, for the elastic case.

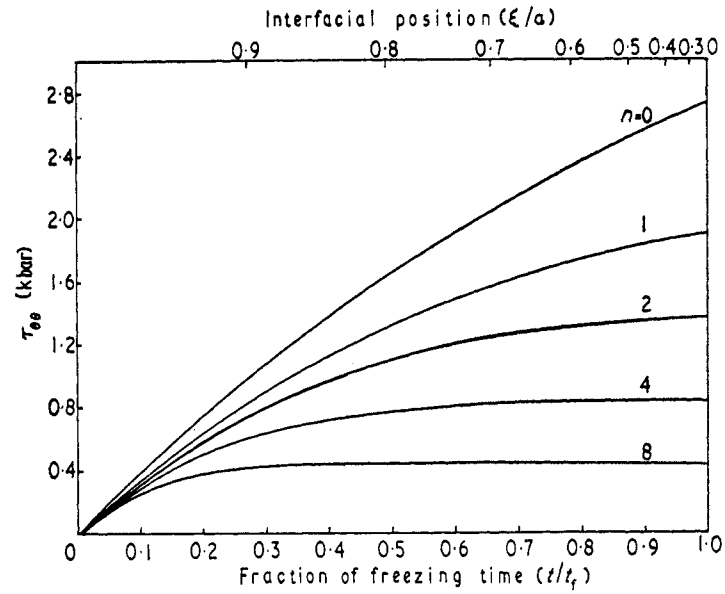

Figure 5. $\tau_{\theta\theta}$ on the surface as a function of time and interfacial position.

(ii) By taking limits as either k or μ tends to zero in equation (25) for the pressure, we can associate each term with a particular mechanical property of the ice. In this way, the first term corresponds to the pressure build-up if the shell were rigid. The second and third terms correspond to elastic movement of the shell in response to the pressure rise, the second being associated with compression, and the third with shearing of the ice.

(iii) On the inner boundary both τ_{rr} and $\tau_{\theta\theta}$ are compressive and equal to the pressure. This is expected since the innermost layer has just grown in equilibrium with that pressure. Both become less compressive towards the outer surface, τ_{rr} decreasing to

zero and $\tau_{\theta\theta}$ becoming tensile. Consequently the shearing stress is zero on the inner boundary and a maximum on the outer. This is in direct contrast to the Lamé treatment, where both $\tau_{\theta\theta}$ and the shearing stresses are a maximum on the inner boundary. Consequently, we would expect cracks to nucleate on the outer boundary, but not necessarily to propagate right through to the inner boundary, since $\tau_{\theta\theta}$ is compressive there.

(iv) Figure 4 shows $\tau_{\theta\theta}$ on the surface as the interface moves in. It rises fairly rapidly, and then levels out as the shell becomes thicker, the compressional stresses on the inside having little effect near the surface.

3. Viscoelastic shell

There is ample experimental evidence that ice creeps appreciably, especially above -20 °C (Jones and Glen 1969, Mellor and Testa 1969, Barnes *et al* 1971), so that any realistic treatment ought to incorporate the effects of this creep. In very broad terms, incorporating creep into an elastic problem effectively makes the shear modulus μ smaller, and we have seen that this could affect the pressure build-up considerably.

For polycrystalline ice under a wide range of stresses, the general behaviour is described by the relation (Barnes *et al* 1971)

$$\dot{\epsilon} \propto [\sinh(\beta\sigma)]^{\nu} \exp(-H/kT)$$

where $\dot{\epsilon}$ is the secondary creep rate in shear, σ the shearing stress, H the activation energy for the process, and β a constant. For stresses below 30 bar, this expression reduces to

$$\dot{\epsilon} \propto \sigma^{\nu} \exp(-H/kT).$$

The exponent ν has been found by various workers to take values lying between 1 and 4 (Jellinek and Brill 1956, Glen 1955). If, as a first approximation, ν is taken as 1, then the deformation corresponds to newtonian viscous flow, with the exponential describing a temperature-dependent viscosity. If the elastic strains are included as well, then the material is known as viscoelastic and the theory developed for the behaviour of such materials can be used. It is only for the case $\nu=1$ that the theory is linear and relatively simple. A solution of the nonlinear problem represented by cases with $\nu>1$ is beyond the scope of our present study.

The differential equations describing the behaviour of a spherical shell of viscoelastic material are as follows. The condition for stress equilibrium remains unchanged as

$$\frac{\mathrm{d}\tau_{rr}}{\mathrm{d}r} = \frac{2}{r}(\tau_{\theta\theta} - \tau_{rr}) \tag{28}$$

as do the defining equations for the strains

$$e_{rr} = \frac{\partial u(r)}{\partial r}$$

$$e_{\theta\theta} = e_{\phi\phi} = \frac{u(r)}{r}. \tag{29}$$

Equations (29) are limited to strains of up to a few per cent, so that useful application can only be made under these limitations.

In ice, as in most materials, the permanent changes in volume are negligible in comparison with the elastic ones, so that an incompressibility condition can be imposed

on the viscous strains, and therefore

$$e_{rr}+2e_{\theta\theta}=\frac{\tau_{rr}+2\tau_{\theta\theta}}{3k} \tag{30}$$

where k is the elastic modulus of compression. Finally we have the flow law

$$\frac{\mathrm{d}}{\mathrm{d}t}(e_{rr}-e_{\theta\theta})=\frac{1}{2\mu}\frac{\mathrm{d}}{\mathrm{d}t}(\tau_{rr}-\tau_{\theta\theta})+\frac{\tau_{rr}-\tau_{\theta\theta}}{2\eta} \tag{31}$$

where η is the effective viscosity.

This equation is a particular form of the generalized relationship between stress and strain for a viscoelastic material which can be written as

$$P\epsilon(t)=Q\sigma(t)$$

where P and Q are differential operators in time, and ϵ and σ are the shearing strains and stresses respectively. The particular equation above refers to a maxwellian material where the total strain is the sum of elastic and viscous components. A higher-order model using Maxwell and Voigt units in combination may be necessary properly to represent ice at very high strain rates, but in the present situation a simple Maxwell unit is adequate. Equations (28)–(31) along with the boundary conditions generalized from (17) as

$$\tau_{rr}(a, t)=0$$

$$\tau_{rr}(\xi(t))=-P(\xi(t))$$

form a set of partial differential equations for the stress and strain fields. Comparison with equations (6)–(9) for the elastic case shows they are identical, except for equation (31) which is a generalized form of equation (8).

This similarity in the differential equations is normally utilized to obtain a correspondence solution to the viscoelastic problem from the previously solved elastic one. Equations (8) and (31) are of the same form if μ is treated as a differential operator in time—ie

$$\mu^{-1}\rightarrow\mu^{-1}+\left(\eta\frac{\mathrm{d}}{\mathrm{d}t}\right)^{-1}.$$

Since there then exists a correspondence between the differential equations, and the boundary and initial conditions are the same, there must be a correspondence between the solutions. Accordingly, the viscoelastic solution is ordinarily obtained by replacing μ^{-1} in the elastic solution with

$$\mu^{-1}+\left(\eta\frac{\mathrm{d}}{\mathrm{d}t}\right)^{-1}$$

and integrating with respect to time from the initial conditions. Provided manipulations of the elastic constants have corresponding permitted manipulations of the operators, the solution so obtained is a valid one.

This method cannot be used in the present problem however. In obtaining the elastic solution, the integration with respect to ξ (effectively one in time) was carried out treating μ as a constant. This integration consequently has an illegal counterpart in the viscoelastic case when μ is a differential operator in time, and the correspondence between the solutions is lost.

Since spatial integrations can be carried out independently of time ones, the correspondence principle can still be used to obtain solutions to the modified Navier equation. In fact, correspondence results could be obtained from any step prior to the first integration in ξ. From the elastic solution (11) we had

$$u(r, \xi)=\frac{f(\xi, a)r}{3k}+\frac{g(\xi, a)}{4\mu r^2}$$

so that the corresponding viscoelastic result is

$$u(r, t)=\frac{f(t)}{3k}r+\frac{g(t)}{4\mu r^2}+\frac{1}{4\eta r^2 \mathrm{d}/\mathrm{d}t}g(t) \tag{32}$$

where the functions f and g depend on t because of the moving boundary. Again, it is the derivatives which are required, and we obtain

$$\frac{\partial u}{\partial t}(r, t)=\frac{r}{3k}\frac{\partial f}{\partial t}+\frac{1}{4\mu r^2}\frac{\partial g}{\partial t}+\frac{1}{4\eta r^2}g(t) \tag{33}$$

$$\frac{\partial \tau_{rr}}{\partial t}(r, t)=\frac{\partial f}{\partial t}-\frac{1}{r^3}\frac{\partial g}{\partial t} \tag{34}$$

$$\frac{\partial \tau_{\theta\theta}}{\partial t}(r, t)=\frac{\partial f}{\partial t}+\frac{1}{2r^3}\frac{\partial g}{\partial t}. \tag{35}$$

The treatment runs parallel to that of the elastic problem. Using the boundary conditions

$$\frac{\partial \tau_{rr}}{\partial t}(a, t)=0 \tag{36}$$

$$\frac{\partial \tau_{rr}}{\partial t}(\xi(t))=-\frac{\mathrm{d}P}{\mathrm{d}t} \tag{37}$$

and

$$\frac{\mathrm{d}P}{\mathrm{d}t}=\frac{-3B}{\xi}\left(\alpha\frac{\mathrm{d}\xi}{\mathrm{d}t}+(1-\alpha)\frac{\partial u}{\partial t}(\xi, t)\right) \tag{38}$$

we obtain the differential equation for $g(t)$:

$$\frac{\mathrm{d}g}{\mathrm{d}t}+\frac{3\kappa}{4\eta}\left[\left(1+\frac{3\kappa}{4\mu}\right)-\left(1-\frac{\kappa}{k}\right)\frac{\xi^3}{a^3}\right]^{-1}g(t)=-3B\alpha\,\xi^2\frac{\mathrm{d}\xi}{\mathrm{d}t}\left[\left(1+\frac{3\kappa}{4u}\right)-\left(1-\frac{\kappa}{k}\right)\frac{\xi^3}{a^3}\right]^{-1} \tag{39}$$

where $\kappa=B(1-\alpha)$.

At this point, it should be noted that $\xi(t)$ is an unknown function of time—a difficulty that was avoided in the elastic problem by making ξ the independent variable. From equation (1), ξ is given by

$$\xi(t)=\zeta(t)+\int_0^t \frac{\partial u}{\partial t}(\xi, t)\,\mathrm{d}t \tag{40}$$

where $\zeta(t)$ is the solution to the uncoupled thermal problem—ie the position of the interface as determined by heat transfer and ignoring the effects of the pressure build-up. Although there is no closed-form solution to this problem (Langford 1967), useful approximations can be made when ice is the shell material because of its relatively high ratio of latent to specific heats (Plooster 1971) and the solution normally used (Johnson

and Hallett 1968) is

$$\zeta(t)=a(1-t/t_f)^{1/3} \tag{41}$$

where t_f is the freezing time of the droplet and is given by

$$t_f=\frac{\rho La^2(1-\Delta Tc/L)}{3mK\Delta T} \tag{42}$$

where ρ is the density of water, L the latent heat of fusion, ΔT the supercooling, c the specific heat of water, K the thermal conductivity of the environment, and m an enhancement factor which incorporates the heat transferred due to convection.

If we use this expression, equations (39) and (40) form a dual set of nonlinear integro-differential equations for $\xi(t)$ and $g(t)$. Rather than attempt to solve this complex problem, we have assumed that, in any time interval, the shell displacements are much less than the inward growth, so that to a sufficient approximation we can write

$$\xi(t)=a\,(1-t/t_f)^{1/3}. \tag{43}$$

The appropriate solution to equation (39) is then given by

$$g(t)=\frac{kB\alpha a^3\,[1-(1+\gamma t/t_f)^{-n}]}{(k-\kappa)n} \tag{44}$$

where

$$\gamma=\frac{4\mu(k-\kappa)}{(3k+4\mu)\kappa} \tag{45}$$

and

$$n=\frac{3\kappa k t_f}{4\eta(k-\kappa)} \tag{46}$$

and is thus the ratio of freezing to viscous relaxation times for the shell.

Using this expression for $g(t)$ gives

$$P(t)=\frac{4\mu kB\alpha}{\kappa\,(4\mu+3k)}\int_0^{\phi}\frac{\phi\mathrm{d}\phi}{(1-\phi)\,(1+\gamma\phi)^{n+1}} \tag{47}$$

where $\phi=t/t_f$. If n is an integer, the integral in (47) can be evaluated in an analytic form, but it must be evaluated numerically for non-integral n. In the limit as n tends to zero, the elastic solution is obtained, and as n tends to infinity, ie the material has zero viscosity, there is no pressure increase.

These results are shown in figure 1. All curves for which the viscous flow is significant ($n\geqslant 4$) have certain features in common: they rise slowly to a value determined by n, maintain this value until freezing is complete, and then rise very sharply. This general behaviour can be divided into three stages: a primary stage in which the shell is thin and essentially still elastic; a secondary stage during which the shell is thicker yet flowing quite easily under the shearing stresses—this is the régime in which the pressure remains fairly constant; and a tertiary stage towards the end of freezing when the interface moves very rapidly and the thick shell is incapable of appreciable distortion.

The stresses in the shell are given by

$$\tau_{rr}(r,t)=-P(r)+\frac{kB\alpha}{k-\kappa}\left(\frac{1}{a^3}-\frac{1}{r^3}\right)\frac{1}{n}\{[1+\gamma\,(1-r^3/a^3)]^{-n}-[1+\gamma t/t_f]^{-n}\} \tag{48}$$

$$\tau_{\theta\theta}(r,t)=-P(r)+\frac{kB\alpha}{k-\kappa}\left(\frac{1}{a^3}+\frac{1}{2r^3}\right)\frac{1}{n}\{[1+\gamma\,(1-r^3/a^3)]^{-n}-[1+\gamma t/t_f]^{-n}\}. \tag{49}$$

These expressions take the form shown in figures 2 and 3 for different values of n.

$\tau_{\theta\theta}$ has its maximum tensile value on the outer surface, where it is given by

$$\tau_{\theta\theta}(a, t) = \frac{1{\cdot}5\, B\alpha k}{(k-\kappa)n}\,[1-(1+\gamma t/t_{\mathrm{f}})^{-n}]. \tag{50}$$

As can be seen from figure 5, it is characterized by a fairly sharp rise at the elastic rate, then a levelling out to a value determined by n.

4. Experiments

The measurements of Visagie (1969) on pressures inside freezing 7 mm drops showed that pressures in excess of 70 bar could be expected. His measurements entailed observing, under a microscope, the deflections of a fine silica U-tube.

For the present set of experiments, a Kulite pressure transducer type YQCS-250-1000 was chosen as the sensor, since it was capable of yielding a continuous record of the pressure curves. This subminiature device consists of a Wheatstone bridge bonded on to a silicon diaphragm, and has an output of 1 mV V^{-1} bar^{-1} in the range 0–140 bar. The sensor was filled with paraffin oil and had a volume of 33 mm^3. The presence of the measuring instrument can obviously have a large effect on the measured pressure, especially towards the completion of freezing when the instrument dead-space volume is approximately equal to that of the unfrozen liquid. Fortunately, the theory can be modified quite simply to incorporate these effects, and is given in the appendix.

Initially a fine silica tube was cemented to the end of the stainless steel sensor to minimize the asymmetry in heat transfer. This was later replaced by a thin-walled stainless steel tube as the silica tended to be broken quite easily. The tube was 0·7 mm in outside diameter with a wall thickness of 0·1 mm. Calculations show that less than 0·1 % of the droplet heat is lost through the tube, so the asymmetry introduced should be negligible. In addition, there was no observable difference in general behaviour for the two types of probes. The bond between the ice and stainless steel was sufficiently good to make it quite difficult to separate the frozen droplet and the probe.

Large drops, usually 1 cm in diameter, were placed at the interface between large volumes of carbon tetrachloride and paraffin oil inside a temperature-controlled chamber. The drop was located using a fine wire ring supported on a silica rod and the sensor was lowered until it was central to the drop. The chamber temperature was lowered to the desired level, and the assumbly left until the drop self-nucleated, the event being marked by a rise in temperature as recorded by a thermocouple placed near the drop. The water used was distilled, de-ionized (resistivity greater than $5 \times 10^4\ \Omega$ m) and vacuum degassed, although the purity and gas content were essentially determined by those of the supporting liquids.

5. Results

A typical curve for a 1 cm diameter drop freezing at -5 °C is shown in figure 6. It shows a calm period after nucleation during which a solid shell forms, followed by a slow build-up of pressure normally associated with the growth of a spike or bulge. These protuberances did not appear to influence subsequent pressure development, since the highest pressure recorded (89 bar) occurred in a droplet with a spike two

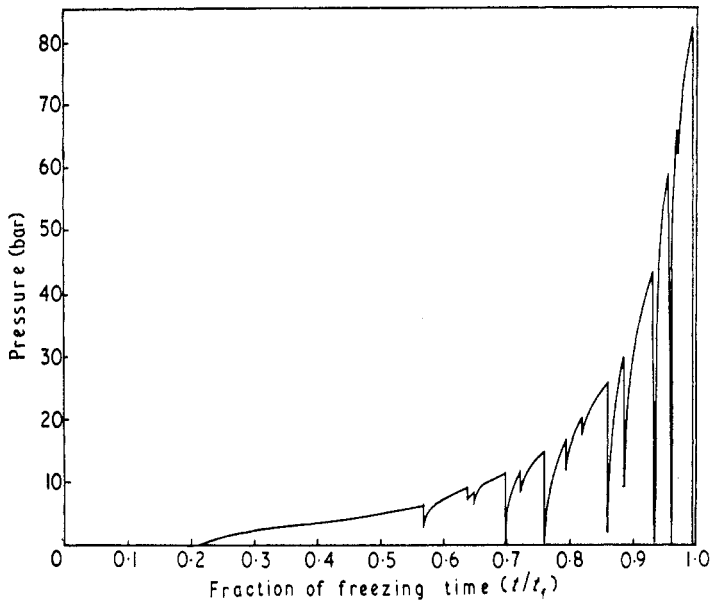

Figure 6. A typical pressure–time record for a drop in diameter 1·1 cm in a bath at temperature −5 °C.

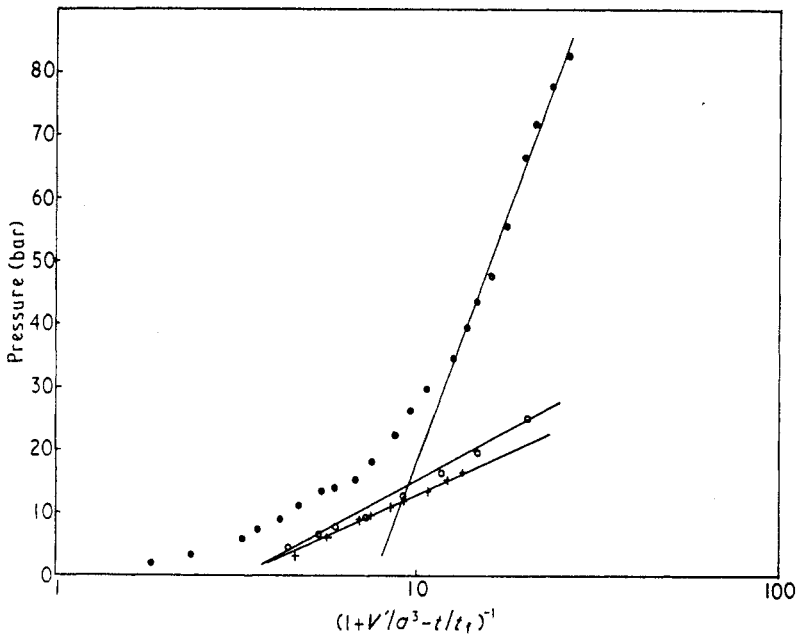

Figure 7. Plot of pressure against lg $(1+V'/a^3-t/t_f)$ for 3 drops:

Symbol	a(mm)	ΔT(K)	t_f(s)
●	5·5	5·0	2180
○	5·0	5·9	2250
+	6·2	8·3	1560

diameters long. This period is followed by one of generally rising pressure broken by up to 50 discontinuities, of which only a small fraction actually decreased to zero, so that not all cracks actually penetrate the shell completely.

After a crack occurs, the record shows that the pressure rises very rapidly back to the value it had previously attained, a feature that analysis shows would be expected for a maxwellian viscoelastic material. Such a material behaves elastically when stresses are applied suddenly, and only exhibits appreciable viscous flow after the stresses have been acting for some time. Consequently, if the stresses in the shell are relieved or partly relieved by a crack, then the pressure will increase at a rate appropriate to an elastic material, and does so until the stresses once again reach the same values they were before the crack occurred.

If one assumes that the envelope represents the pressure development in the absence of cracks, then it should follow the result derived in the appendix, which incorporates the effect of the instrument. Accordingly a plot of P against lg $(1+V'/a^3-t/t_t)$ should be a straight line with a slope of $4\mu kB\alpha\,[\kappa\,(4\mu+3k)\,(1+\gamma)^{n+1}]^{-1}$, particularly near the completion at freezing.

The results for three droplets freezing in different conditions are shown in figure 7 yielding values for n of 5·9, 5·3, and 3·6. Using these values of n and equation (46), we obtain values for the effective viscosity η of $5{\cdot}3\times10^{11}$, $7{\cdot}8\times10^{11}$, and $6{\cdot}6\times10^{11}$ N m^{-2} s.

These values can be compared with the creep measurements of Barnes *et al* (1971). If we define the effective viscosity in this case by η = applied stress/creep rate, then their measurements yield an effective viscosity of $2{\cdot}8\times10^{10}$ N m^{-2} s at an applied stress of 10 bar, and $1{\cdot}4\times10^{14}$ N m^{-2} s at 1 bar. The stress in our experiment is of the order of 10 bar, so the effective viscosity is within an order of magnitude of the macroscopic value, which is all that can be expected in view of the linear approximation made in the theory.

The assumption of a linear dependence of strain rate on stress is also responsible for the high predicted values of surface stress. Figure 4 shows that, for values of n between 3 and 5, the theory predicts $\tau_{\theta\theta}\,(a)$ to have the value of 600 bar. In view of the fact that the ultimate tensile strength of ice is approximately 20 bar over a wide range of strain rates (Hawkes and Mellor 1972), the discrepancy between the actual and predicted stress distributions is considerable. If the strain rate depended on a higher power of the stress, however, much lower stresses would be sufficient to give appreciable strain rates.

Droplets that froze when the chamber temperature was warmer than −2·8 °C exhibited no appreciable pressure increase. Under these conditions, equation (38) shows that the strain rate is approximately given by

$$\dot{\epsilon}=\frac{-\alpha}{(1-\alpha)\,a}\frac{\mathrm{d}\xi}{\mathrm{d}t}.$$

For the droplets considered, this corresponds to a strain rate of approximately 10^{-5} s^{-1}. Using the experimental creep data of Barnes *et al* (1971) we find that this strain rate requires an applied stress of 20 bar. Since it is difficult to reconcile a stress of 20 bar in the shell with zero pressure in the core, it appears that even nonlinear secondary creep rates cannot be used to explain this aspect. It would appear then that transient creep processes are also important, and should be incorporated in any treatment which attempts to predict realistic stress distributions.

About 20% of the droplets measured contained a residual pressure of typically

10–20 bar at the completion of freezing. This pressure decayed with a time constant of about 200 s, and it is tempting to ascribe this decay to viscous relaxation of the frozen droplet; but a simple analysis shows that the time constant for this process is too large by four orders of magnitude. It is also unlikely that it can be attributed to the sensor oil leaking out through a microcrack, since for a time constant of 200 s it has to be 1 μm wide, and it is difficult to envisage conditions under which cracks of these dimensions could form without resealing.

We attribute this decay to the decrease in temperature of the drop after freezing is complete. During the freezing process, the temperature of the liquid core remains close to 0 °C, decreasing to the chamber temperature only after the droplet has completely frozen. The relative difference in thermal expansion between paraffin oil and ice would then serve to reduce the pressure. Calculations show that this would lead to a decrease of 9 bar K^{-1}. Comparison of the decay curves with the temperature as monitored near the surface of the drop yielded an average decay rate of 5 bar K^{-1}. Since the temperature at the centre of the drop will lag behind that on the surface, the agreement is reasonable.

6. Conclusions

It is clear that the theory predicts experimental pressure developments reasonably well. The stress distribution is not so realistic, but it could be improved by taking a nonlinear flow law, and by incorporating the effects of transient creep. Any such treatment must still retain the elastic strains since these are important during the initial stages of freezing and in the processes following the occurrence of a crack. A treatment incorporating these effects is essential before one can use the theory to predict quantitatively the cracking behaviour of cloud-size droplets, for, without a reliable stress distribution, one has no effective criterion for determining the onset of cracking. Despite these difficulties, we can, however, make certain general statements about the likelihood of shattering under different conditions.

Equations (42) and (46) show that for cloud-size droplets in the size range 50–500 μm and freezing between 0° and −20 °C, the parameter n can vary over three orders of magnitude. Within this broad range, we can say that the large drops freezing at warmer temperatures will exhibit appreciable viscous flow, and the smaller ones freezing at cooler temperatures will exhibit more elastic behaviour and crack more often. Between these two extremes, there is probably a size and temperature range in which sufficient elastic energy is stored in the shell to shatter it violently, but the theory is unable to predict these important ranges. The presence of dissolved gases in the water would have little overall effect on this picture, as their incorporation as bubbles in the ice shell would tend to have a uniform weakening effect.

The numerous discontinuities in the pressure curves indicate that large-scale movements of the ice shell occur many times during the freezing of a droplet, and these could be a source of ice particles even when the droplet does not shatter. Careful experiments would be needed to examine this possibility, as these particles would probably be micron-sized, and their detection requires special experimental techniques.

Realistic predictions of the cracking activity of cloud-size droplets will therefore require a more refined theory and more detailed experimental investigations on the size and temperature dependence of this activity.

Acknowledgments

This work is part of a project supported by the Australian Research Grants Committee. One of us (W D K) is also grateful to the CSIRO for a scholarship.

Appendix. The effect of instrument volume on measured pressures

Suppose that the instrument is filled with oil of volume V_0 and bulk modulus B_0, and that the measurement of pressure occurs at a time when the volume of the liquid core is V_W. If the volume of the liquid core is changed by δV_W, then the increase in pressure δP is given by

$$\delta P = -\frac{B\delta V_W}{V_W + BV_0/B_0}. \tag{A1}$$

Equation (38) can then be modified to

$$\frac{dP}{dt} = -\frac{3B\alpha\xi^2}{\xi^3 + V'}\left(\alpha\frac{\partial\xi}{\partial t} + (1-\alpha)\left.\frac{\partial u}{\partial t}\right|_{\xi}\right) \tag{A2}$$

where $V' = 3BV_0/4\pi B_0$. In proceeding along the same lines as before, we obtain the differential equation

$$\frac{dg}{dt}\left[\left(\frac{\xi^3}{a^3}\right)^2\left(1-\frac{\kappa}{k}\right) + \frac{\xi^3}{a^3}\left(\frac{V'}{a^3} - 1 - \frac{3\kappa}{4\mu}\right) + \frac{V'}{a^3}\right] - \frac{3\kappa}{4\eta}\frac{\xi^3}{a^3}g(t) = \frac{3B\alpha}{a^3}\xi^5\frac{d\xi}{dt} \tag{A3}$$

for which the solution is

$$g(t) = \frac{\Lambda}{n}\left[1 - \left(\frac{l(1-\phi)^2 + s(1-\phi) + q}{l+s+q}\right)^{-n/2}\left(\frac{(2l(1-\phi)+s+\Delta)(2l+s-\Delta)}{(2l(1-\phi)+s-\Delta)(2l+s+\Delta)}\right)^{-sn/2\Delta}\right] \tag{A4}$$

where $\phi = t/t_f$, $\Lambda = kB\alpha^3/(k-\kappa)$, $l = 1-\kappa/k$, $q = V'/a^3$, $s = V'/a^3 - 1 - 3\kappa/4\mu$, and $\Delta = (s^2 - 4lq)^{1/2}$.

For the droplets considered, $V'/a^3 < 0{\cdot}1$, so that the approximation $\Delta = s$ can be made, and then $g(t)$ reduces to

$$g(t) = \frac{kB\alpha a^3}{(k-\kappa)n}\left[1 - (1+\gamma t/t_f)^{-n}\left(1 - \frac{V'}{a^3}\frac{4\mu}{(4\mu+3\kappa)}\right)^{-n/2}\right]. \tag{A5}$$

Comparison with equation (44) shows that $g(t)$ is only slightly reduced. This result could have been anticipated, since the problem is such that $g(t)$ is determined by the processes at the commencement of freezing when the effects of the measuring instrument are only slight.

Using this expression for $g(t)$ gives

$$\frac{dP}{dt} = \frac{4\mu kB\alpha}{(3k+4\mu)\kappa t_f}\left(1 - \frac{4\mu V'}{a^3(4\mu+3\kappa)}\right)^{-n/2}\left(\frac{1}{(1+V'/a^3-\phi)(1+\gamma\phi)}\right)^{(1+\gamma\phi)^{n+1}} \tag{A6}$$

and

$$P = \frac{4\mu kB\alpha}{\kappa(3k+4\mu)}\left(1 - \frac{4\mu V'}{a^3(4\mu+3\kappa)}\right)^{-n/2}\int_0^{\phi}\frac{d\phi}{(1+\gamma\phi)^{n+1}(1+V'/a^3-\phi)}. \tag{A7}$$

The factor $\{1-4\mu V'/[a^3(4\mu+3\kappa)]\}^{-n/2}$ is small, giving a correction of less than 20% for $n < 10$. It is very sensitive to changes in n compared with the factor $(1+\gamma\phi)^{-n-1}$ and was neglected in analysing the data.

The integral is such that the major contribution to it comes from the last stages of freezing as $\phi \rightarrow 1$, where it can be approximated by $(1+\gamma)^{-n-1} \lg (1+V'/a^3-\phi)$ and this is the relationship used in analysing the data.

References

Barnes P, Tabor D and Walker J C F 1971 *Proc. R. Soc.* A **324** 127–55
Brownscombe J L and Thorndike N S C 1968 *Nature, Lond.* **220** 687–9
Glen J W 1955 *Proc. R. Soc.* A **228** 519–38
Gold L W 1958 *Can. J. Phys.* **36** 1265–75
Hawkes I and Mellor M 1972 *J. Glaciol.* **11** 103–31
Hobbs P V and Alkezweeny A J 1968 *J. atmos. Sci.* **25** 881–8
Jellinek H H G and Brill R 1956 *J. appl. Phys.* **27** 1198–209
Johnson D A and Hallett J 1968 *Q. J. R. Meteorol. Soc.* **94** 468–82
Jones S J and Glen J W 1969 *J. Glaciol.* **8** 463–73
Langford D 1967 *Q. appl. Math* **24** 315–22
Mellor M and Testa R 1969 *J. Glaciol.* **8** 147–52
Mossop S C 1970 *Bull. Am. Meteorol. Soc.* **51** 474–9
Plooster M N 1971 *J. atmos. Sci.* **28** 1299–301
Sokolnikoff I S 1956 *Mathematical Theory of Elasticity* (New York: McGraw-Hill)
Visagie P J 1969 *J. Glaciol.* **8** 301–9